Journal of Chromatography A, 1545 (2018) 84–92

Contents lists available at ScienceDirect

Journal of Chromatography A

journal homepage: www.elsevier.com/locate/chroma

# Separating large microscale particles by exploiting charge differences with dielectrophoresis☆

Danielle V. Polniak, Eric Goodrich, Nicole Hill, Blanca H. Lapizco-Encinas*

*Microscale Bioseparations Laboratory and Biomedical Engineering Department, Rochester Institute of Technology, Rochester NY, USA*

ARTICLE INFO

*Article history:*
Received 9 December 2017
Received in revised form 18 February 2018
Accepted 24 February 2018
Available online 24 February 2018

*Keywords:*
Dielectrophoresis
Electric field
Electrophoresis
Electrokinetics
Electrical charge
Microparticles

ABSTRACT

Dielectrophoresis (DEP), the migration of particles due to polarization effects under the influence of a nonuniform electric field, was employed for characterizing the behavior and achieving the separation of larger (diameter >5 μm) microparticles by exploiting differences in electrical charge. Usually, electrophoresis (EP) is the method of choice for separating particles based on differences in electrical charge; however, larger particles, which have low electrophoretic mobilities, cannot be easily separated with EP-based techniques. This study presents an alternative for the characterization, assessment, and separation of larger microparticles, where charge differences are exploited with DEP instead of EP. Polystyrene microparticles with sizes varying from 5 to 10 μm were characterized employing microdevices for insulator-based dielectrophoresis (iDEP). Particles within an iDEP microchannel were exposed simultaneously to DEP, EP, and electroosmotic (EO) forces. The electrokinetic behavior of four distinct types of microparticles was carefully characterized by means of velocimetry and dielectrophoretic capture assessments. As a final step, a *dielectropherogram* separation of two distinct types of 10 μm particles was devised by first characterizing the particles and then performing the separation. The two types of 10 μm particles were eluted from the iDEP device as two separate peaks of enriched particles in less than 80 s. It was demonstrated that particles with the same size, shape, surface functionalization, and made from the same bulk material can be separated with iDEP by exploiting slight differences in the magnitude of particle charge. The results from this study open the possibility for iDEP to be used as a technique for the assessment and separation of biological cells that have very similar characteristics (shape, size, similar make-up), but slight variance in surface electrical charge.



## 1. Introduction

There is an increasing demand for miniaturized systems that provide inexpensive, portable and easy-to-use avenues for biological sample analysis. Microfluidics is a rapidly growing field that can satisfy these demands and takes advantage of the benefits of working on the microscale, such as low sample and reagent consumption, rapid response times, and increased resolution and sensitivity. Important efforts are dedicated towards the continued development of analytical and separation techniques that are suitable for miniaturization.

Electrokinetics (EK), a family of phenomena that depend on the electrical double layer, is one of the main pillars of microfluidics, due to its simplicity and ease in application. Electric-field driven techniques, such as electroosmosis (EO), electrophoresis (EP) and dielectrophoresis (DEP), have been successfully used for the analysis, sorting, and separation of a wide array of bioparticles in microfluidic devices. These applications range from environmental assessments [1–3] to biomedical and clinical analyses [4–6]. In such systems, EO flow is usually employed to pump liquid and particles through the microchannels, eliminating the need for external pumping mechanisms or moving parts. Furthermore, in microscale EK systems many charged particles will also experience EP motion under the influence of electric fields [7,8]. Separation of particles employing electric fields can be achieved by the simultaneous control of EO and EP effects, as particles with distinct charge magnitude will migrate at different velocities. There are numerous successful reports in the literature on the separation of nano-bioparticles, such as proteins and DNA [9–11]. However, separating larger particles (diameter >1 μm) via electrophoresis can be challenging due to

☆ Selected paper from the 24th International Symposium on Electro- and Liquid Phase-Separation Techniques (ITP2017), 10–13 September 2017, Sopot, Poland.

* Corresponding author at: Micoscale Bioseparations Laboratory, Rochester Institute of Technology, Institute Hall (Bldg. 73), Room 3103 160 Lomb Memorial Drive, Rochester, NY, USA.
*E-mail address:* bhlbme@rit.edu (B.H. Lapizco-Encinas).

https://doi.org/10.1016/j.chroma.2018.02.051
0021-9673/

their low charge to mass ratio, which results in low electrophoretic mobilities, in many cases, much lower than the EO mobility.

Separation of larger particles, such as bacteria and other microbes, with EP techniques was proposed by Hjerten et al. in 1987 [12] and reported for the first time by Ebersole and McCormick in 1993 [13]. Two research groups in particular have made several significant contributions to this field. The first group, Armstrong and collaborators published a series of reports on the separation of microbes employing electrophoretic techniques. Specifically, the excellent article published in 1999 [14] demonstrated that intact biological cells could be efficiently separated by employing techniques usually limited to macromolecules. In this study, a combination of capillary electrophoresis (CE) and capillary isoelectric focusing (CIEF) were employed for the separation and identification of seven distinct species of microbes (six bacteria and one yeast species) with a wide array of sizes and shapes. To achieve successful separations, polyethylene oxide (PEO) was used as EO flow suppressant, since the EO mobility can be much greater than EP mobility for biological cells. All reported separation took less than 20 min. The resulting electropherograms had excellent resolutions (good peak shape) and efficiencies as high as 1,600,000 plates per meter were reached [14]. One significant advantage of these types of electrophoretic separations is that several parameters can be exploited: particle size, shape, and surface charge. This work was later extended for the identification of bacterial pathogens responsible for urinary tract infections, with analysis times below 10 min and efficiencies in the range of one million plates per meter [15]. Furthermore, by combining CE with laser-induced fluorescence, Armstrong and He [16] were able to successfully assess cell viability with automated UV detection, opening the opportunity for high throughput analysis. This approach was also extended to food analysis [17], where the rapid quantification of the total number of live cells in a food sample was demonstrated, highlighting the potential of these techniques for applications in regulatory agencies and food safety analysis. CE coupled with fluorescence was also used for monitoring migration behavior of microorganisms, allowing for observation of the separation process and identification of optimal operating conditions [18], as well as the dynamics behind microbe focusing effects and cell aggregation [19]. More recent applications reported by Armstrong's group include the detection of bacterial contamination, where CE offers a much quicker alternative to traditional methods (minutes vs. weeks) [20] and an enhanced sensitivity for sterility tests [21], including characterization of surfactants used to enhance bacterial detection [22]. Even bacterial phenotype has been assessed employing CE methodologies [23].

The second group that has led several significant advances on the use of CE for bacterial manipulation, enrichment, and separation is Buszewski and collaborators. In 2003, they reported the separation of bacteria by CE [24], much like Armstrong's findings [14]. In order to enhance the EP mobility of the cells, EO flow was suppressed by employing γ-(trimethoxysilyl)propyl methacrylate followed by acrylamide. They were able to determine the EP mobility for four distinct bacterial species as well as the analysis of peak shape for *E. coli* under a range of buffer pH and ionic strength. The separation of a mixture containing all four distinct types of bacteria was achieved in less than eight minutes employing an 8.5 cm long capillary with a 75 μm diameter and suppressed EO flow. This group continued this work with the successful separation of four bacterial species employing PEO and EO flow suppressant and capillaries modified with divinylbenzene or trimethylchlorosilane [25]. The separation time was shortened to 5 min for four bacterial species and eight minutes for five species in an 8.5 cm long capillary with high EP mobilities. This work was later extended to highly pathogenic species such as *E. coli* (urinary tract infections) and *Helicobacter pylori* (stomach colonization) [26,27]. They reported the successful enrichment and detection of *E. coli* for direct urine samples with capillary zone electrophoresis (CZE) in less than 14 min and identification of *H. pylori* aggregates in less than 35 min. These findings demonstrate the great potential of electromigration techniques for the diagnosis of microbe-based illnesses [28]. Further work on CZE illustrated that monolith beds could also be used for the separation of pathogenic bacteria [29]; and that CZE separations could be validated with molecular methods [30]. The option of using in line fluorescence detection with a stereomicroscope employing a short 2 mm long capillary further demonstrated the applicability of CE as an analytical technique for microbes [31]. An excellent report in 2009 summarized the distinct approaches of electromigration techniques for the separation of intact cells [32]. More recent reports by this group have studied the dynamics of bacterial aggregates, with impressive separation times under five minutes. Their findings included the effects of modification of bacterial surface with calcium ions, and the focusing of bacterial aggregates by performing the separation in an isotachophoretic mode. An excellent recent review on the use of electromigration techniques for microbiological and clinical applications is available in this reference [33].

The use of CE or CZE techniques for the rapid detection and assessment of intact cells keeps gaining momentum as EP-based techniques offer an efficient, robust, and much more rapid alternative for cell analysis compared to traditional techniques. CZE has been used for viability assessments with potential application in food analyses [34]. Other new reports have focused on high speed CE separations with short-end capillaries, where the identification of oral bacteria was achieved in 95 s [35]. These types of separations can also be carried out in capillaries etched with critical water, as demonstrated with the use of CZE to separate antibiotic resistant bacteria from prepared laboratory samples [36] and infected whole human blood [37].

However, in some cases, electrophoretic separations are not feasible for particles and cells that are weakly charged, neutral, or have very similar charge to others present in the sample. In addition, some of the EP-based cell separations mentioned above required the addition of chemicals to suppress EO flow, either by coating capillaries or by adding a reagent to the running buffer [14–19,24–29]; these reagents could alter cell characteristics, since PEO, for example, can be used to inhibit bacterial aggregation [38]. An alternative to EP-based separations is to employ DEP, which is the motion of polarizable particles (neutral or charged) toward or away from regions of high electric field gradients under the effects of a nonuniform electric field [39]. The net dielectrophoretic particle motion is the result of the interaction of the induced multipole experienced by the particles and the nonuniform electric field [40]. Furthermore, particles can exhibit positive or negative dielectrophoretic behavior. Positive DEP is when particles migrate towards strong electric field regions and negative DEP is when particles move away from these regions [41]. DEP also offers additional flexibility, since DEP is more strongly dependent on the field gradient rather than on field magnitude. Thus, it can be applied employing direct current (DC) and/or alternating current (AC) electric fields.

The two most popular methods of DEP are electrode-based DEP (eDEP) and insulator-based DEP (iDEP); the former is when microelectrodes are used to create the required nonuniform electric fields, and the latter is when insulating structures are used for the same purpose [42–44]. An advantage of iDEP over eDEP, is that insulating structures provide a truly 3-dimensional dielectrophoretic effect, since usually insulators transverse the entire height of the microchannel or chamber. Planar electrodes, which are common in eDEP, have the disadvantage that the dielectrophoretic force acting on the particles decreases rapidly as it moves away from the

electrode surface. Therefore, planar electrodes are limited to low throughput applications [1]. The fabrication of 3-dimensional electrodes circumvents this limitation. So and Dickey [45] employed low melting point alloys (eutectic gallium indium, EGaln) injected directly into the microfluidic channel to create 3-dimensional electrode structures that allow for direct contact between the electrodes and the fluid. These electrodes transverse the entire channel depth, similar to iDEP systems. They employed PDMS posts spread out along the channel between the electrodes and the channel to keep the liquid metal from entering the channel. This study provides a novel technique for microelectrode fabrication that does not require any soldering. The authors demonstrated the utility for electrohydrodynamic mixing rather than for DEP [45]. Tang et al. [46] reported the rapid creation of Galinstan microstructures with various dimensions and aspect ratios. These 3-dimensional microelectrodes were employed to enhance the trapping of tungsten trioxide nanoparticles with DEP. This provided an advantage over the standard planar electrode arrays, since microelectrodes stand at a height of 50 μm, creating a true 3-dimensional dielectrophoretic effect.

The effect of particle surface characteristics on DEP has been extensively studied for sub-micron particles [41,47–49]. Fewer studies have focused on larger particles, such as biological cells. Betts and Brown deliver an excellent overview of the theory behind dielectrophoresis. In particular they describe how differences in surface characteristics of the cells can be exploited for identifications and separation purposes [50]. This group has studied DEP for applications in water and food analysis and developed microsystems for effective cell quantification for protozoa [51,52]. Fernandez et al. [53] published a recent excellent review on the application of DEP for microbial analysis. In this extensive report, the authors cover the fundamentals of microbial polarization as well as enhanced DEP-based systems for the detection of microbes that range from immuno-capture to PCR amplification [53].

In the present study, differences in electrical charge were exploited in order to achieve effective separation of larger microscale particles by means of iDEP, that is, charge differences were assessed with DEP instead of traditional EP techniques. Since iDEP exploits both charge and polarization effects, it offers an additional alternative for separating larger microparticles (diameter >5 μm). A large majority of DEP-based studies that have exploited particle size, shape, and polarizability differences have focused on the separation of "smaller" particles (diameter <5 μm) [54–57]. In this study we examined the EK behavior of polystyrene microparticles with diameters ranging from 5 to 10 μm by employing DC electric fields with iDEP microchannels. All particles utilized had a negative carboxyl surface modification that allowed for EP motion towards the channel inlet, and the analysis was performed in the presence of EO flow toward the channel outlet. We selected these "larger" microparticles as they can be representative of biological cells with distinct surface charge characteristics. The results illustrated that it is possible to effectively separate particles that have the same size, shape, same type of surface functionalization, and are made from the same bulk material (polystyrene), but differ slightly in the magnitude of their surface charge. A mixture of two distinct, but very similar, types of 10 μm particles was characterized and then separated. These particles were the same size, same type of surface functionalization, and were made from the same substrate material, differing only in the magnitude of their surface charge. These two types of particles were selectively eluted from the iDEP device by varying the applied electrical potential; this separation was illustrated as a *dielectropherogram* depicting two distinct peaks of enriched particles. This study opens the possibility for iDEP to be used as technique for the assessment and separation of biological cells that have very similar characteristics, but may vary slightly in their surface properties, such as different make-up of the membranes, *i.e.* transmembrane proteins.

## 2. Theoretical background

The dielectrophoretic force exerted on a spherical particle depends on particle and suspending medium properties, as well as on the electric field gradient:

$$\vec{F}_{DEP} = 2\mu\varepsilon_m r_p^3 Re\,(f_{CM})\,\nabla E^2 \tag{1}$$

where $\nabla E^2$ refers to the gradient of the electric field squared. Particle polarizability is expressed through the $f_{CM}$ which accounts for the complex permittivities of the particle and the suspending medium [40]:

$$f_{CM} = \left(\frac{\varepsilon_p^* - \varepsilon_m^*}{\varepsilon_p^* + 2\varepsilon_m^*}\right) \tag{2}$$

where $\varepsilon^* = \varepsilon - \left(j\sigma/\omega\right)$, while σ and ε are real conductivity and permittivity values, respectively, ω is the angular frequency of the applied electric potential, and $j = \sqrt{-1}$. For spherical particles the magnitude of the $f_{CM}$ ranges from −0.5 to 1.0 [40]. In this study, due to their large size, all particles had negative DEP behavior (*i.e.*, negative $f_{CM}$ value). Particles with diameter >500 nm will always exhibit negative dielectrophoretic behavior under DC or low frequency AC fields [49] due to their thin EDL compared to particle radius. A thin EDL leads to negligible electrophoretic contribution to the particle's dipole moment and overall low particle conductivity, which in turn produces a negative $f_{CM}$ value [49,58]. The expression for the dielectrophoretic velocity of a particle ($\vec{v}_{dep}$), as function of the dielectrophoretic mobility ($\mu_{dep}$) is:

$$\vec{v}_{dep} = \mu_{dep}\nabla E^2 = \frac{r_p^2\varepsilon_m}{3\eta} Re\,[f_{CM}]\,\nabla E^2 \tag{3}$$

where η is the viscosity of the suspension medium. In addition to the DEP velocity, particle migration in iDEP systems depends on the EK velocity. EK migration is the superposition of EP and EOF effects, which in turn depend on the $\zeta_{particle}$ and $\zeta_{wall}$ values, respectively.

$$\vec{v}_{ek} = -\frac{\varepsilon_m\left(\zeta_{wall} - \zeta_{particle}\right)}{\eta}\vec{E} \tag{4}$$

In this study, all particles exhibit a net EK motion towards the outlet reservoir, since the magnitude of $\zeta_{wall}$ (−81.57 mV) has a greater magnitude than that of $\zeta_{particle}$ (Table 1, −39.95 to −66.53 mV). An expression for a particle net velocity ($\vec{v}_p$), which depends on $\vec{v}_{dep}$ and $\vec{v}_{ek}$, can be written as:

$$\vec{v}_p = (\mu_{EO} + \mu_{EP})\,\vec{E} + \mu_{dep}\nabla E^2 = -\frac{\varepsilon_m\left(\zeta_{wall} - \zeta_{particle}\right)}{\eta}\vec{E} + \frac{r_p^2\varepsilon_m}{3\eta} Re\,[f_{CM}]\,\nabla E^2 \tag{5}$$

where $\mu_{EP}$ and $\mu_{EO}$ are the electrophoretic and electroosmotic mobilities, respectively.

## 3. Materials and methods

### 3.1. Microdevices

Experiments were conducted in microchannels with insulating posts made from polydimethylsiloxane (PDMS) employing standard soft lithography techniques [59]. To create a device, PDMS (Dow Corning, Midland, MI) is cast onto a negative replica mold made with a silicon wafer (Silicon Inc., Boise, ID) and SU-8 3050

**Table 1**
Characteristics of the fluorescent polystyrene microspheres used in this study. Zeta potential values were experimentally measured in our laboratory.

| Diameter (μm) | Color (Ex/Em) | Functionality | $\zeta_{particle}$ (mV) | Concentration (Particles/mL) | Type of experiment |
|---|---|---|---|---|---|
| 5.0 | Red (538/584) | Carboxyl | −47.92 ± 2.17 | $1.46 \times 10^7$<br>$3.64 \times 10^5$ | Minimum voltage for trapping<br>iDEP velocimetry |
| 7.6 | Green (475/540) | Carboxyl | −47.49 ± 5.72 | $6.22 \times 10^6$<br>$2.69 \times 10^5$ | Minimum voltage for trapping<br>iDEP velocimetry |
| 10 | Green (475/540) | Carboxyl | −39.95 ± 1.90 | $2.18 \times 10^6$<br>$1.88 \times 10^5$ | Minimum voltage for trapping<br>iDEP velocimetry |
| 10 | Red (580/605) | Carboxyl | −66.53 ± 1.28 | $2.18 \times 10^6$<br>$1.82 \times 10^5$ | Minimum voltage for trapping<br>iDEP velocimetry |
| 10/10 Mixture | Green (475/540) Red (538/584) | Carboxyl | – | $5.91 \times 10^6$<br>$5.89 \times 10^6$ | Dielectropherogram separation |

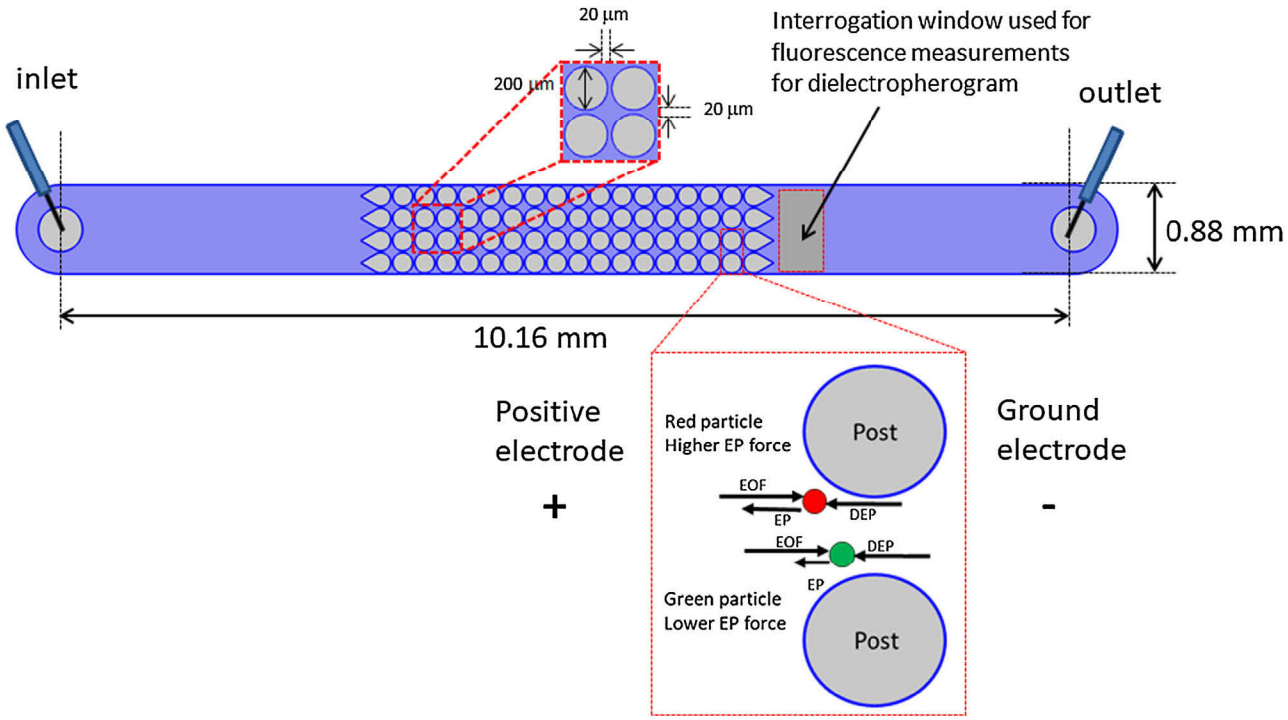


**Fig. 1.** **(a)** Schematic representation of the iDEP channel employed in this study. **(b)** Representation of the forces acting on the particles where the EP force acting on the red particles has a greater magnitude than the EP force acting on the green particles. (For interpretation of the references to colour in this figure legend, the reader is referred to the web version of this article.)

photoresist (MicroChem, Newton MA). After the PMDS is thermally cured at 85 °C for 40 min and 135 °C for 5 min, the PDMS slab is removed from the mold and inlet/outlet liquid reservoirs are punched. A 4 in glass wafer covered with a thin layer of PDMS is then used to seal the channel by employing a plasma corona wand (Electro Technic Products, Chicago, IL) which activates both PDMS surfaces. The PDMS slab is pressed against the PDMS-covered glass wafer, creating microchannels where all internal surfaces are PDMS and have same wall zeta potential ($\zeta_{wall}$), ensuring consistent EO flow. The microchannels were 10.16 mm long, 0.88 mm wide, 40 μm deep and contained one inlet and one outlet liquid reservoir. The dimensions of the circular posts employed were 200 μm in diameter and arranged in a square array of 220 μm center-to-center. The array of insulating structures consisted of 72 posts located at the center of the channel in an 18 × 4 post arrangement (Fig. 1a). Particle image velocimetry measurements (PIV) were carried out employing a 30.48 mm long microchannel fabricated in the same manner (image not shown). The PIV devices did not contain any insulating posts. Current monitoring assessments were performed employing plain channels (with no posts) in triplicate (image not shown), using three channels in parallel to allow for enhanced signal to noise ratio, as reported in one of our previous studies [60] (Fig. 2).

### 3.2. Microparticles

For experimentation four distinct types of fluorescent carboxylated polystyrene microspheres of three different sizes were employed. All of these particles had a negative carboxyl surface functionalization with varying charge magnitude (Table 1). Particle zeta potential was experimentally measured in our laboratory by combining PIV measurements performed in a plain channel and current monitoring assessments [60]. Briefly, particle electrokinetic mobility was estimated with PIV, then fluid electroosmotic mobility was measured with current monitoring. From this data, particle EP mobility and particle zeta potential ($\zeta_{particle}$) were estimated. Particle concentrations for all iDEP experiments are listed in Table 1.

### 3.3. Equipment and software

Microparticle behavior was observed and recorded in the form of videos and pictures with a ZEISS Axiovert 40 CFL inverted

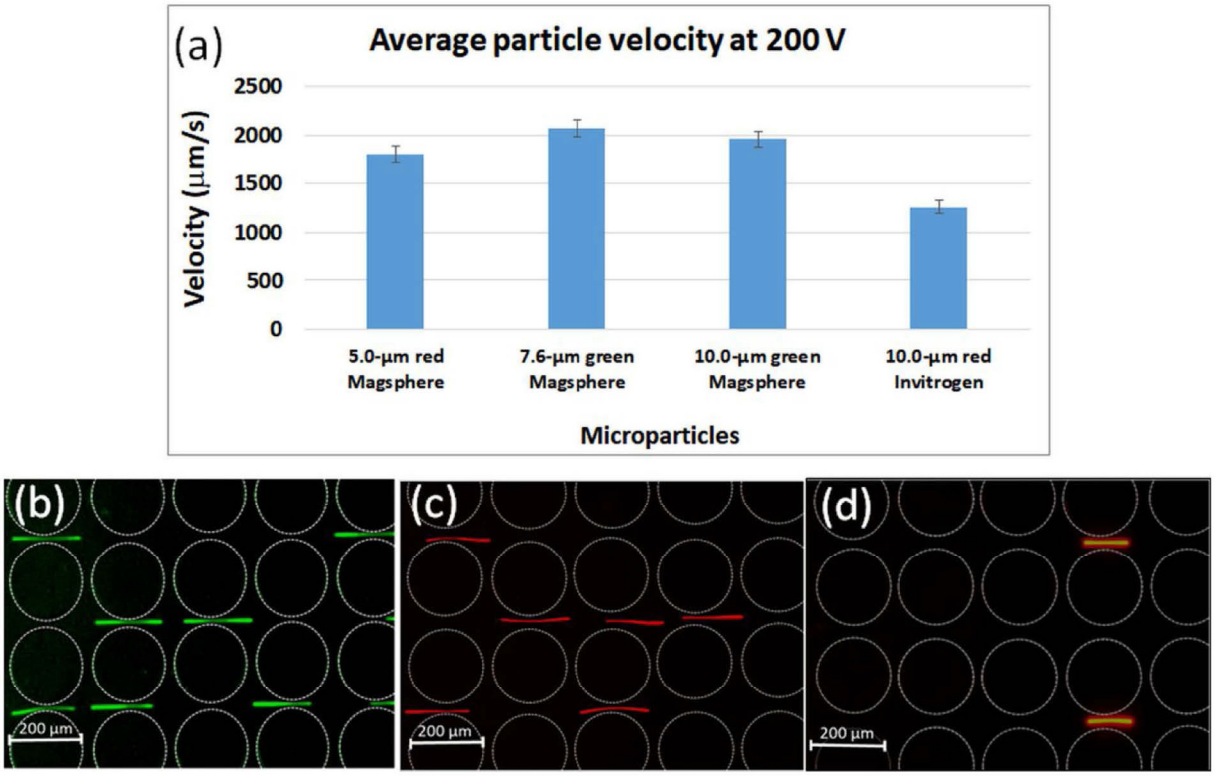


**Fig. 2.** **(a)** Particle streak line velocimetry measurements in an iDEP microdevice at an applied voltage of 200 V. Examples of streak lines used for velocimetry assessments are shown in: **(b)** 10 μm Magsphere particles at 500 V, **(c)** 5-μm Magsphere particles at 500 V, and **(d)** 10 μm Invitrogen particles at 300 V. (For interpretation of the references to colour in this figure legend, the reader is referred to the web version of this article.)

microscope (Carl Zeiss Microscopy, Thornwood, NY) paired with an Infinity 2 camera (Lumenera, Ottawa, Canada) and the software *Infinity Capture* provided by the manufacturer. The separation of the two distinct types of 10 μm particles was visualized with a Leica DMi8 inverted microscope (Wetzlar, Germany) that was paired with a Leica DFC7000 T camera and the software *LASX* provided by the manufacturer. A personal computer was required to operate the voltage sequencer and two microscopes. Direct current (DC) electric potentials were applied across the length of the channel by employing the high voltage supply (Model HVS6000D, LabSmith, Livermore, CA). The voltage sequencer was manipulated with the software *Sequence* provided by the manufacturer. COMSOL *Multiphysics* 4.4 was used to model particle velocities between constrictions (see Fig. 3b). Full model details can be found in the supplementary information file.

### 3.4. Suspending media

The suspending medium employed for experiments had a conductivity of 15–20 μS/cm and a pH of 6–7. This suspending medium consisted primarily of deionized (DI) water with Tween 20 added at a concentration of 0.05% (v/v) to minimize particle aggregation and sticking to channel walls. A 0.1 M KCl solution and a 0.1 M KOH solution were used to adjust the medium conductivity and pH to the desired values. Nine different particle suspensions were made of varying concentrations ($1.8 \times 10^5$–$1.5 \times 10^7$ particles/mL) based on size and type of experiment: minimum trapping voltage or velocimetry assessment (see Table 1). Particle image velocimetry and current monitoring measurements employed a suspending medium with similar pH and conductivity that also contained 0.05% (v/v) Tween 20. Dielectropherogram experiments required a slightly higher surfactant concentration (0.5% (v/v) Tween 20) to prevent enriched particles from agglomerating.

### 3.5. Experimental procedure

All iDEP experiments started with a clean PDMS device that contained 14 microchannels that were preconditioned by soaking them in the suspension medium to activate the zeta potential of the PDMS surface and ensure stable EO flow. All particle samples were sonicated for 10 min to break aggregates prior to experimentation. The channels were sealed to a vacuum chunk manifold (LabSmith, Livermore, CA) with a vacuum pump. The manifold interfaced with slip tip syringes for easy filling of the microchannels with pressure. After the channel was attached to the manifold, a sample of 10–20 μL of the selected particle suspension was added to the channel inlet and platinum wire electrodes were placed in the channel reservoirs. After eliminating any present pressure-driven flow, a DC electric potential was applied across the length of the channel by employing the high voltage supply. Particle response was recorded in the form of pictures and videos that were used for further analysis.

For iDEP streak line velocimetry experiments, the particle samples were exposed to applied voltages between 200 and 500 V and recorded using the microscope and video camera under an exposure time of 70 ms for a period of 20–30s. The videos of the each microparticle sample were analyzed with FIJI/IMAGEJ software [61] by employing the straight line interrogation option across a number of particle streak lines to measure the length in pixels. This value was multiplied by a predetermined μm to pixel ratio of 0.9 μm/pixel, based on the use of 10 x microscope objective to visualize and capture the experiments. This average length in μm was divided by the exposure time of 70 ms to get an average velocity measurement of each particle type within the iDEP microchannel.

During minimum trapping experiments the applied voltage was varied between 100 and 1400 V until there was observable trapping of several particles. For the particle separation experiment, initial

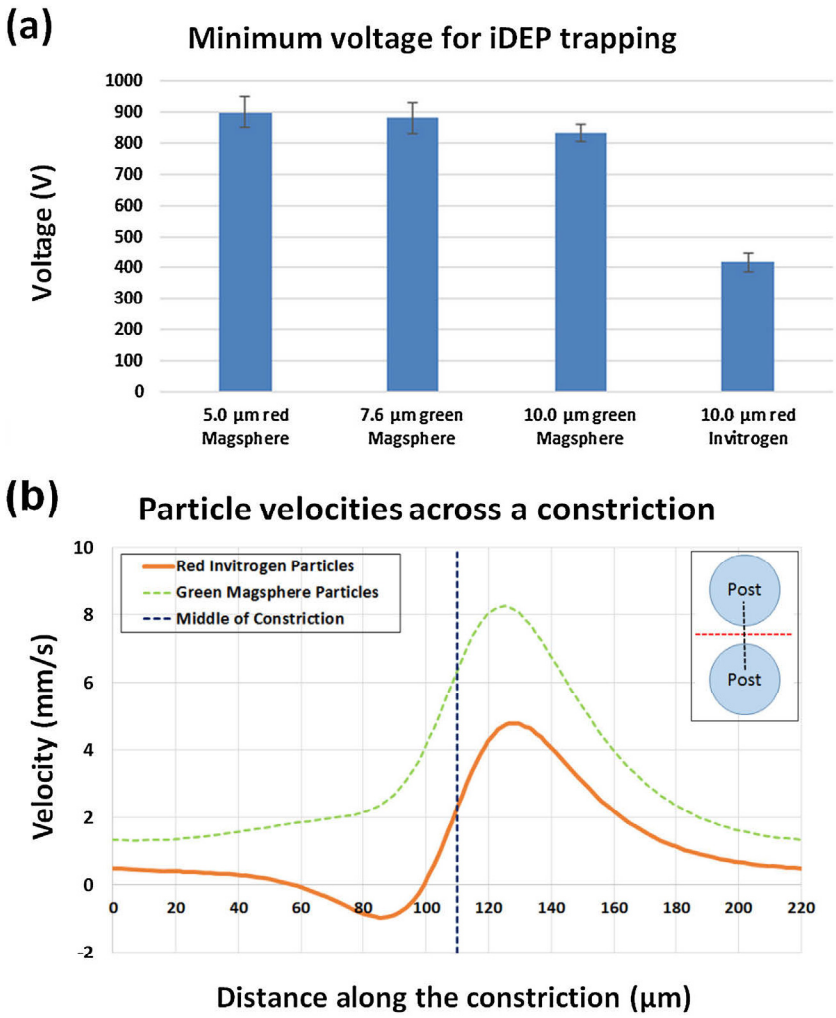


**Fig. 3.** **(a)** Characterization of the minimum DC electric voltage required to achieve particle trapping within the iDEP microchannel. **(b)** Predicted particles velocities across one constriction between two posts at 500 V. The inset of the top right corner depicts the location of the cutline (in red color) used for these predictions. Particle surface charge differences result in a change in the electrophoretic mobility and velocity, as reflected in the overall particle velocity. Red particles are trapped at this potential, as illustrated by their overall velocity which reaches negative values. (For interpretation of the references to colour in this figure legend, the reader is referred to the web version of this article.)

assessment of the behavior of the mixture of two distinct types of 10 μm particles was performed, followed by the dielectropherogram. Separation was obtained by selectively releasing one particle type at a time by applying a set of voltage steps, where each was held for a predetermined amount of time (see Fig. 4d).Videos of the particles being released and crossing the interrogation window for fluorescence measurements (see Fig. 1a) were analyzed with *FIJI/IMAGEJ* software [61] by measuring the integrated density of the differently fluorescing particles to track the release rates of the different particles. The fluorescence measurements were employed to create the dielectropherogram using Microsoft Excel.

## 4. Results and discussion

### 4.1. Characterization of particle velocity

Effect of charge on particle velocity was explored through three different experiments: PIV, current monitoring, and streak line velocimetry. Current monitoring experiments [60] allowed for the determination of the $\zeta_{wall}$ of the PDMS devices and the EO mobility of the selected suspending medium, yielding values of −81.57 mV and $6.36 \times 10^{-8}$ m$^2$/V s, respectively. These results were used in combination with PIV measurements to determine particle EP mobility and $\zeta_{particle}$. As can be seen in Table 1, all particles have a negative $\zeta_{particle}$ value, which is expected due to their negative carboxyl functionality. Red Invitrogen particles, 10 μm in diameter, had the highest charge magnitude (highest $\zeta_{particle}$ magnitude). For all particles, the magnitude of $\zeta_{wall}$ was greater than the magnitude of $\zeta_{particle}$, therefore all particles had an overall EK migration towards the outlet reservoir, meaning all moved from positive to negative (from left to right in our images). Fig. 1b illustrates the forces acting on the particles, for the purpose of this image the two types of 10 μm particles were included, where red 10 μm particles have a stronger EP force acting on them.

Streak line particle velocimetry within an iDEP microchannel was employed to characterize particle motion under the combination of DEP, EP and EO forces. Under the influence of DC and low frequency AC electric fields all polystyrene particles with diameter larger than 500 nm exhibited negative DEP behavior regardless of the magnitude the particle surface charge [62]. Particles exhibiting negative DEP slow down prior to crossing a constriction between two insulating posts due to repulsive DEP forces [56]. Velocimetry measurements were performed using particle streak lines as the particles crossed the constrictions between the cylindrical posts (see Experimental Section for details). Fig. 2a shows the velocity results for all four types of particles tested in this study at an applied

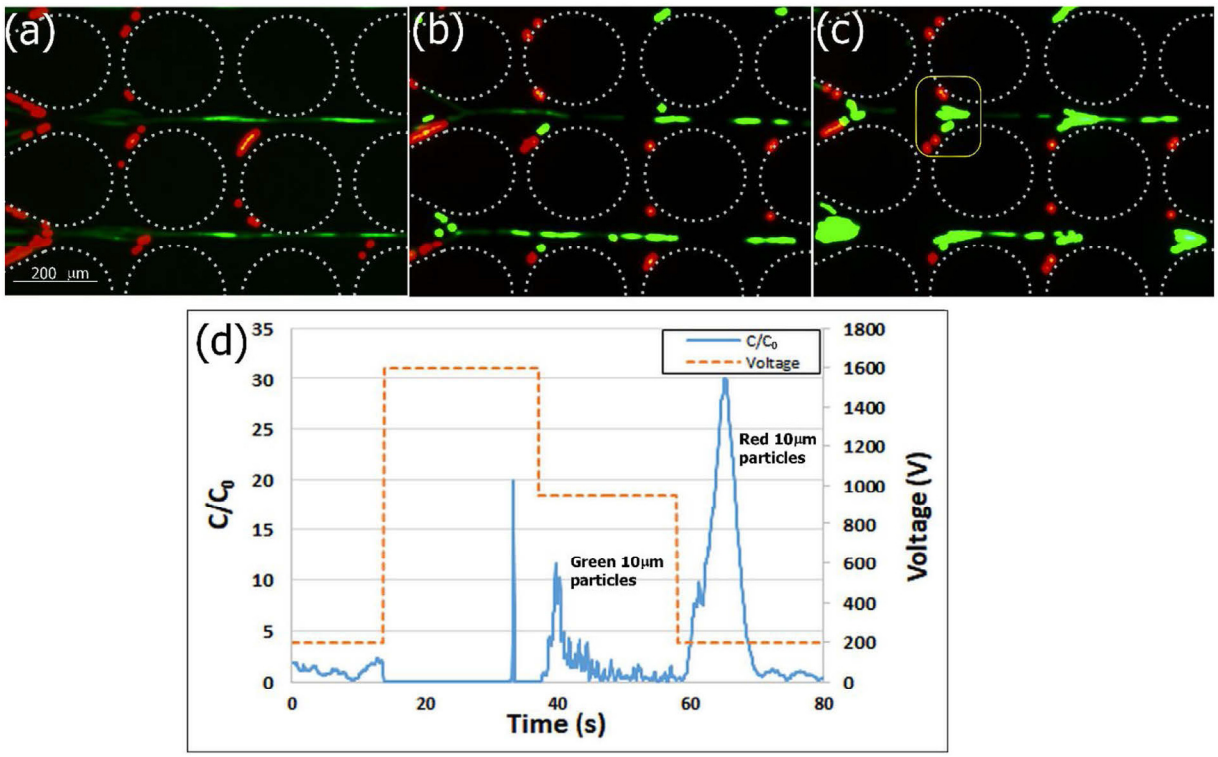


**Fig. 4.** Experimental separation of two distinct types of 10 μm carboxylated polystyrene particles by exploiting charge difference. **(a)** At 500 V the red Invitrogen particles are trapped, while the green Magsphere particles continue to flow. **(b)** At 800 V the red Invitrogen particles are trapped, while the green Magsphere particles are partially trapped. **(c)** At 900 V both types of particles are trapped, but the green Magsphere particles are trapped closer to the constrictions (see rectangle within the image), illustrating spatial separation between the two types of trapped particles. **(d)** Dielectropherogram showing the separation of the two types of 10 μm particles eluted as two separated peaks of enriched particles, fluorescence measurements were employed to illustrate particle enrichment. The first peak shows elution of the lower charged 10 μm green Magsphere particles, while the second, broader and larger peak shows elution of the higher charged 10 μm red Invitrogen particles. Fluorescence measurements ($C$) are normalized by the initial fluorescence in the system ($C_0$) measured during the first 10 s where no particle trapping was present. These two types of 10 μm particles have the same size, same shape, same type of surface functionalization, and are made from the same substrate material. (For interpretation of the references to colour in this figure legend, the reader is referred to the web version of this article.)

DC voltage of 200 V. As it can be observed 10 μm red particles from Invitrogen, which have a high surface charge (Table 1), have the lowest overall particle velocity within the iDEP channel. Since EO migration is the same for all particles, these results can be explained as function of two mechanisms: the strong EP migration of these highly negative charged particles towards the inlet and the effect of this high charge on the negative dielectrophoretic mobility of the particles, which is also towards the inlet. As mentioned in the Theory section, due to their large size, for all particles studied here, the electrophoretic contribution to particle polarization is negligible and all particles will exhibit a negative $f_{CM}$ [49,58] which leads to negative DEP. Furthermore, for the conditions of this study, of thin EDL and DC potentials, the particle's dipole moment is governed by ion transport between the EDL and the bulk solution. According to the Dukhin–Shilov model, the particle's EDL is in equilibrium with the bulk solution at low frequencies since the ions have sufficient time to migrate. Zhao [58] explains that at low frequencies, there is a complex relationship between $\zeta_{particle}$ and the dipole coefficient. The particles in this study have a normalized $|\zeta|$ values (normalized with thermal voltage of ~25 mV) below 3.0, for these conditions Zhao's predictions produce a slightly lower magnitude $f_{CM}$ for the particles with the highest charge (10 μm red Invitrogen particles) [58]. This means that dielectrophoretic force exerted on the particles with the most charge is slightly lower than that exerted on the other particles. However, this effect on particle polarization is not as significant as the effect of the EP motion, which explains why the particles with the highest surface charge have the lower overall particle velocity. Fig. 2b–d illustrate examples of the images used for these velocimetry assessments. Numerous experiments were performed for velocimetry measurements with applied voltages between 200 and 500 V. At these voltages, DEP is only strong enough to influence particle migration (streaming iDEP [63]), so particles are continuously flowing and not trapped by DEP effects.

As seen in Fig. 2a, the lower charged 10 μm Magsphere green particles were migrating at almost 2000 μm/s near the center of the constrictions while the higher charged 10 μm Invitrogen particles were travelling at around 1200 μm/s. There is a significant velocity difference despite the very similar characteristics of these two distinct types of particle. These results clearly illustrate the potential of iDEP to be used as a separation technique for very similar particles types: both types of 10 μm particles have the same size, shape, type of surface charge (carboxyl), and are made from polystyrene. Figs. 2b–d depict the type of streak lines that were ideal for measurements. These streak lines are clear and do not overlap. It is important to note that 5 μm and 7.6 μm Magsphere particles, which possess a lower charge, are also migrating at a higher velocity than the higher charged Invitrogen particles.

### 4.2. Characterization of the minimum voltage required for particle dielectrophoretic trapping

The behavior of these four types of larger microparticles was also assessed in terms of the minimum voltage required to achieve particle trapping in an iDEP microchannel. Our group has reported this type of particle characterization in previous studies [64]. The aim was to analyze the effect of particle electrical charge on dielectrophoretic particle capture/trapping. The experimental results, plotted in Fig. 3a, clearly demonstrate that the three types of Mag-

sphere particles, which have lower surface charge, require higher voltages (~doubled magnitude) to "trap" than the highly charged 10 μm Invitrogen particle. The Magsphere particles of three different sizes trapped at voltages ranging from 800 to 950 V, with the 5 μm red particles requiring the most at 900–950 V. The highly charged 10 μm Invitrogen particles began trapping at voltages around 400–450 V, half of that required for any of the Magsphere particles. From the perspective of DEP, which scales with particle volume, it makes sense that 5-μm and 7.6-μm particles require a higher applied voltage, since they are smaller than the 10 μm particles. It is interesting to note that two types of 10 μm particles that are the same size, same shape, and made from the same substrate material (polystyrene) behave so differently. While the Magsphere particles have $\zeta_{particle}$ values within the −40 mV range, the highly charged Invitrogen particles have a $\zeta_{particle}$ value near the −60 mV range. The particles with a higher magnitude of negative $\zeta_{particle}$ experience a larger EP force toward the inlet, which aids the negative DEP force in trapping particles (*i.e.*, the larger the magnitude of the negative $\zeta_{particle}$, the easier it is for DEP to capture and trap particles within the array of posts). Particle size is supposed to be the dominant parameter when it comes to dielectrophoretic particle manipulation (Eq. (1), DEP force depends on particle volume); however, the results in Fig. 3a clearly illustrate that particle surface charge ($\zeta_{particle}$) also plays an important role on particle behavior in iDEP systems. To further illustrate the effects of particle electrical charge on dielectrophoretic response, a COMSOL model was built to predict the overall particle velocity as function of EP, EO and DEP. These results are plotted in Fig. 3b. Under negative DEP, particles slow down prior to each construction. In this case, the overall particle velocity (Eq. (5)) for the red 10 μm particles crosses the zero velocity value as they slow down; producing particle trapping prior to the center of the constriction (illustrated by the black dotted line). In contrast, the green 10 μm particles never reach the zero velocity value when they slow down, thus, no trapping of the green 10 μm particles is observed. A potential of 500 V was selected for this simulation, as it is slightly over the minimum trapping voltage (Fig. 3a) which ensures that all red particles should be trapped. This potential of 500 V also agrees with the results in Fig. 4a that show trapping of red 10 μm particles.

### 4.3. Dielectropherogram: separation of two distinct types of similar 10 μm particles

This observation was further explored through a mixture separation experiment where the two distinct types of 10 μm microparticles were employed. The microspheres were the same size, shape, bulk material, and had the same type of carboxyl surface functionalization. However, the magnitude of the carboxyl charge on their surfaces differed. As mentioned prior, the 10 μm green Magsphere particles were considered to have a lower charge than the 10 μm red Invitrogen particles (Table 1, $\zeta_{particle}$ values). The DEP response of a mixture of the two distinct types of 10 μm particles, which can be seen in Fig. 4a, shows that at an applied DC voltage of 450–500 V the higher charged red 10 μm particles were captured at the constrictions between the cylindrical posts, while the green 10 μm particles, which bear lower charge, continued to flow. Figs. 4b and c further confirm these observations. Fig. 4b shows 10 μm green particles starting to trap and Fig. 4c depicts full dielectrophoretic capture of both types of 10 μm particles. In Fig. 4c it is observed that the 10 μm green particles are captured closer to the constriction between the posts while the 10 μm red particles are captured at a location further upstream (see constriction marked with a yellow rectangle). Particles in iDEP systems are captured at locations where the different forces exerted on the particles are at equilibrium; from the results we can gather that these two distinct types of 10 μm particles have different equilibrium locations under the employed experimental conditions. These results were used to design a dielectropherogram separation, which consists of the dielectrophoretic capture of all particles present in a sample by applying a high voltage, followed by the selective release of one particle type at a time. Our group has pioneered this type of dielectrophoretic separations [64–66]. As mentioned in the materials and method section, fluorescence signals from the eluting particles are recorded just downstream from the post array (see Fig. 1a). The fluorescence readings were analyzed with *FIJI/IMAGEJ* software [61]. Fluorescence values ($C$) are normalized to the initial fluorescence ($C_0$) of the system, taken from the average fluorescence over the first ten seconds; in this case, particle concentration was equated to fluorescence intensity. Fig. 4d shows the concentration of the eluting particles as function of time and applied voltage. As observed, particles were eluted as two distinct peaks; some leakage of green particles is observed at ~35 s, and the peak came at ~38 s, followed by a very well-defined peak for red particles at ~60 s. Besides being separated, both particles types were enriched, one fold for green particles, while red particles were enriched 30 times their initial concentration. The entire separation was achieved in ~80 s. These results demonstrate that iDEP can be used for the simultaneous separation and enrichment of larger particles (diameter >5 μm) by exploiting differences on electrical charge, a parameter usually exploited in electrophoretic-based separations.

## 5. Concluding remarks

The migration of larger (diameter >5 μm) microparticles in an iDEP system is not only affected by their size and shape, but also by the magnitude of their surface electrical charge. This study analyzed larger polystyrene microparticles of varying sizes (5–10 μm) that featured a negative carboxyl surface functionalization and were tested in the presence of EO flow. Particle behavior was first characterized by employing velocimetry assessments, which showed that surface charge had a significant effect on particle velocity within an iDEP channel. Particles were also studied in terms of the minimum DC voltage required to achieve particle trapping within an iDEP device. These results also confirmed that the effects of electrical charge on the dielectrophoretic trapping of particles were significant, perhaps as significant as the effect of particle size. The latter was surprising, as DEP force scales with particle volume and traditionally particle size has been considered the main parameter dominating particle behavior in iDEP systems. These results also illustrate that it is possible for 10 μm particles to be dielectrophoretically captured at the same voltage of 5 μm particles, regardless of the significant volume difference.

The results obtained by employing a mixture of two distinct types of 10 μm particles further strengthen the concept that the magnitude of the electrical charge of the particles plays a major role in dielectrophoretic separations. It is possible to select specific applied voltages at which one type of particle will be captured with DEP while the other type of particle continues to flow along with the liquid, regardless of the many similarities between the two types of particles. The dielectropherogram separation clearly illustrates that it is possible to separate particles that are the same size, shape, have same type of surface functionalization, and are made from the same material, by exploiting slight differences in electrical charge. This is similar to EP-based separations that are based on charge differences. These results open the potential for applications of iDEP that involve the separation of biological cells that have very similar characteristics and may vary slightly on their surface properties, such as different make-up of their cell membranes, *i.e.* transmembrane proteins. This study also demonstrates that iDEP can be used as an alternative to electrophoresis for achieving particle and cell separations by exploiting surface charge differences.

## Acknowledgement

The authors would like to acknowledge the financial support provided by the National Science Foundation (Awards CBET-1336160 and CBET- 1705895).

## Appendix A. Supplementary data

Supplementary data associated with this article can be found, in the online version, at https://doi.org/10.1016/j.chroma.2018.02.051.

## References

[1] N.M. Jesús-Pérez, B.H. Lapizco-Encinas, Electrophoresis 32 (2011) 2331.
[2] A.G. Crevillén, M. Hervás, M.A. López, M.C. González, A. Escarpa, Talanta 74 (2007) 342.
[3] C.B. Freitas, R.C. Moreira, M.G. de Oliveira Tavares, W.K.T. Coltro, Talanta 147 (2016) 335.
[4] A. Sonnenberg, J.Y. Marciniak, J. McCanna, R. Krishnan, L. Rassenti, T.J. Kipps, M.J. Heller, Electrophoresis 34 (2013) 1076.
[5] N. Abd Rahman, F. Ibrahim, B. Yafouz, Sensors 17 (2017) 449.
[6] T.A. Douglas, J. Cemazar, N. Balani, D.C. Sweeney, E.M. Schmelz, R.V. Davalos, Electrophoresis 38 (2017) 1507.
[7] J.J. Zhu, X.C. Xuan, J. Colloid Interface Sci. 340 (2009) 285.
[8] K. Dorfman, in: D. Li (Ed.), Encyclopedia of Microfluidics and Nanofluidics, Springer, US, 2008, p. 580.
[9] M.C. Breadmore, Electrophoresis 28 (2007) 254.
[10] L.D. Garza-García, V.H. Pérez-González, O.A. Pérez-Sánchez, B.H. Lapizco-Encinas, Chem. Eng. Technol. 34 (2011) 371.
[11] M. Ramos-Payán, J.A. Ocaña-Gonzalez, R.M. Fernández-Torres, A. Llobera, M. Ángel Bello-López, Electrophoresis 39 (2017) 111.
[12] S. Hjertén, K. Elenbring, F. Kilár, J.-L. Liao, A.J.C. Chen, C.J. Siebert, M.-D. Zhu, J. Chromatogr. A 403 (1987) 47.
[13] R.C. Ebersole, R.M. McCormick, Nat. Biotechnol. 11 (1993) 1278.
[14] D.W. Armstrong, G. Schulte, J.M. Schneiderheinze, D.J. Westenberg, Anal. Chem. 71 (1999) 5465.
[15] D.W. Armstrong, J.M. Schneiderheinze, Anal. Chem. 72 (2000) 4474.
[16] D.W. Armstrong, L.F. He, Anal. Chem. 73 (2001) 4551.
[17] D.W. Armstrong, J.M. Schneiderheinze, J.P. Kullman, L.F. He, FEMS Microbiol. Lett. 194 (2001) 33.
[18] M. Girod, D.W. Armstrong, Electrophoresis 23 (2002) 2048.
[19] D.W. Armstrong, M. Girod, L.F. He, M.A. Rodriguez, W. Wei, J. Zheng, E.S. Yeung, Anal. Chem. 74 (2002) 5523.
[20] M.A. Rodriguez, A.W. Lantz, D.W. Armstrong, Anal. Chem. 78 (2006) 4759.
[21] A.W. Lantz, Y. Bao, D.W. Armstrong, Anal. Chem. 79 (2007) 1720.
[22] Y. Bao, A.W. Lantz, J.A. Crank, J. Huang, D.W. Armstrong, Electrophoresis 29 (2008) 2587.
[23] A.W. Lantz, B.F. Brehm-Stecher, D.W. Armstrong, Electrophoresis 29 (2008) 2477.
[24] B. Buszewski, M. Szumski, E. Klodzinska, H. Dahm, J. Sep. Sci. 26 (2003) 1045.
[25] M. Szumski, E. Klodzinska, B. Buszewski, J. Chromatogr. A 1084 (2005) 186.
[26] E. Klodzinska, H. Dahm, R. Rózycki, J. Szeliga, M. Jackowski, B. Buszewski, J. Sep. Sci. 29 (2006) 1180.
[27] B. Buszewski, E. Klodzinska, H. Dahm, H. Rózycki, J. Szeliga, M. Jackowski, Biomed. Chromatogr. 21 (2007) 116.
[28] M. Jackowski, J. Szeliga, E. Klodzinska, B. Buszewski, Anal. Bioanal. Chem. 391 (2008) 2153.
[29] B. Buszewski, E. Klodzinska, Electrophoresis 29 (2008) 4177.
[30] K. Hrynkiewicz, E. Klodzinska, H. Dahm, J. Szeliga, M. Jackowski, B. Buszewski, FEMS Microbiol. Lett. 286 (2008) 1.
[31] M. Szumski, E. Klodzinska, B. Buszewski, Microchim. Acta. 164 (2009) 287.
[32] E. Klodzinska, B. Buszewski, Anal. Chem. 81 (2009) 8.
[33] B. Buszewski, E. Kłodzińska, TrAC-Trend. Anal. Chem. 78 (2016) 95.
[34] F. Crispo, A. Capece, A. Guerrieri, P. Romano, LWT – Food Sci. Technol. 68 (2016) 506.
[35] J. Chen, Y. Ni, C. Liu, Y. Yamaguchi, Q. Chen, S. Sekine, X. Zhu, X. Dou, Talanta 160 (2016) 425.
[36] M. Horká, P. Karásek, F. Růžička, M. Dvořáčková, M. Sittová, M. Roth, Anal. Chem. 86 (2014) 9701.
[37] M. Horká, M. Tesařová, P. Karásek, F. Růžička, V. Holá, M. Sittová, M. Roth, Anal. Chim. Acta 868 (2015) 67.
[38] A. Roosjen, H.C. van der Mei, H.J. Busscher, W. Norde, Langmuir 20 (2004) 10949.
[39] H.A. Pohl, Dielectrophoresis, Cambridge University Press, Cambridge, 1978.
[40] T.B. Jones, Electromechanics of Particles, Cambridge University Press, New York, USA, 1995.
[41] H. Morgan, N.G. Green, AC Electrokinetics: Colloids and Nanoparticles, Research Studies Press LTD, Hertfordshire, England, 2003.
[42] R. Pethig, J. Electrochem. Soc. 164 (2017) B3049.
[43] K. Khoshmanesh, S. Nahavandi, S. Baratchi, A. Mitchell, K. Kalantar-zadeh, Biosens. Bioelectron. 26 (2011) 1800.
[44] B. Çetin, D. Li, Electrophoresis 32 (2011) 2410.
[45] J.-H. So, M.D. Dickey, Lab Chip 11 (2011) 905.
[46] S.-Y. Tang, J. Zhu, V. Sivan, B. Gol, R. Soffe, W. Zhang, A. Mitchell, K. Khoshmanesh, Adv. Funct. Mater. 25 (2015) 4445.
[47] N.A.M. Yunus, H. Nili, N.G. Green, Electrophoresis 34 (2013) 969.
[48] S. Basuray, H.-C. Chang, Phys. Rev. E 75 (2007) 060501.
[49] M. Romero-Creel, E. Goodrich, D. Polniak, B. Lapizco-Encinas, Micromachines 8 (2017) 239.
[50] W.B. Betts, A.P. Brown, J. Appl. Microbiol. 85 (1999) 201S.
[51] W.B. Betts, Trends Food Sci. Technol. 6 (1995) 51.
[52] C.M. Quinn, G.P. Archer, W.B. Betts, B. O'Neill, in: W.B. Betts, D.P. Casemore, C.R. Fricker, H.V. Smith, J. Watkins (Eds.), Protozoan Parasites and Water, Royal Society of Chemistry, Cambridge, 1995, p. 125.
[53] R.E. Fernandez, A. Rohani, V. Farmehini, N.S. Swami, Anal. Chim. Acta 966 (2017) 11.
[54] K.H. Kang, X. Xuan, Y. Kang, D. Li, J. Appl. Phys. 99 (2006) 064702.
[55] R. Riahifar, E. Marzbanrad, B. Raissi, C. Zamani, M. Kazemzad, A. Aghaei, Mater. Lett. 65 (2011) 632.
[56] M.A. Saucedo-Espinosa, B.H. Lapizco-Encinas, Electrophoresis 36 (2015) 1086.
[57] M.A. Saucedo-Espinosa, M.M. Rauch, A. LaLonde, B.H. Lapizco-Encinas, Electrophoresis 37 (2016) 635.
[58] H. Zhao, Phys. Fluids 22 (2010) 072004.
[59] D.C. Duffy, J.C. McDonald, O.J. Schueller, G.M. Whitesides, Anal. Chem. 70 (1998) 4974.
[60] M.A. Saucedo-Espinosa, B.H. Lapizco-Encinas, Biomicrofluidics 10 (2016) 033104.
[61] J. Schindelin, I. Arganda-Carreras, E. Frise, V. Kaynig, M. Longair, T. Pietzsch, S. Preibisch, C. Rueden, S. Saalfeld, B. Schmid, J.-Y. Tinevez, D.J. White, V. Hartenstein, K. Eliceiri, P. Tomancak, A. Cardona, Nat. Meth. 9 (2012) 676.
[62] M.E. Arsenault, H. Zhao, P.K. Purohit, Y.E. Goldman, H.H. Bau, Biophys. J. 93 (2007) L42.
[63] E.B. Cummings, IEEE Eng. Med. Biol. Mag. 22 (2003) 75.
[64] A. LaLonde, A. Gencoglu, M.F. Romero-Creel, K.S. Koppula, B.H. Lapizco-Encinas, J. Chromatogr. A 1344 (2014) 99.
[65] H. Moncada-Hernández, B.H. Lapizco-Encinas, Anal. Bioanal. Chem. 396 (2010) 1805.
[66] A. Gencoglu, D. Olney, A. LaLonde, K.S. Koppula, B.H. Lapizco-Encinas, Electrophoresis 35 (2014) 363.